

Non Equilibrium Transitions in a Polymer Replication Ensemble

Arthur Genthon,¹ Carl D. Modes,^{2,3,4} Frank Jülicher,^{1,3,4} and Stephan W. Grill^{2,3,4}

¹Max Planck Institute for the Physics of Complex Systems, 01187 Dresden, Germany

²Max Planck Institute for Molecular Cell Biology and Genetics, 01307 Dresden, Germany

³Center for Systems Biology Dresden, 01307 Dresden, Germany

⁴Cluster of Excellence, Physics of Life, TU Dresden, 01307 Dresden, Germany

The fuel-driven process of replication in living systems generates distributions of copied entities with varying degrees of copying accuracy. Here we introduce a thermodynamically consistent ensemble for investigating universal population features of replicating systems. In the context of copolymer copying, coarse-graining over molecular details, we establish a phase diagram of copying accuracy. We discover sharp non-equilibrium transitions between populations of random and accurate copies. Maintaining a population of accurate copies requires a minimum energy expenditure that depends on the configurational entropy of copolymer sequences.

Introduction - The ability to replicate is a hallmark of the living world. For example, organisms can replicate themselves, as well as cells, and the long polymeric molecule DNA [1]. Generating a DNA polymer copy with near-identical sequence to the template DNA requires energy consumption [2, 3]. DNA replication is catalyzed by the molecule DNA polymerase, which progressively moves along the template DNA strand as it generates a polymer copy [4]. Generating copies of DNA competes with DNA disassembly, catalyzed for example by DNAses without involvement of a fuel [5]. Detailed models have been used to discuss the key properties of this copy process, typically focusing on individual replicates of a template sequence [6–17]. This provided insights onto the fundamental limits and trade-offs associated with polymer replication. Examples of this include trade-offs [11, 15, 18] and correlations [14] between speed, accuracy and cost of replication; links between dissipation, elongation and information transmission [6, 8]; and definitions of replication efficiency [13].

Here we investigate the conditions for establishing whole populations of accurate copies of a copolymer template. In order to focus on generic features, we coarse-grain molecular details of copying such as sequential steps of initiation [16], polymer elongation [6, 9] and strand separation [13, 17] into a one-step stochastic process. We define what we call a replication ensemble where a single template in presence of reservoirs of fuel and monomers generate a population of stochastic copies. We study the distribution of copying errors as a function of copying specificity and active driving by the fuel. We establish a phase diagram of copying accuracy for the replication ensemble, and discover sharp transitions between populations of random and accurate copies in the limit of long polymers. Our replication ensemble allows for a thermodynamic description of non-equilibrium steady-state populations of accurate and random polymer copies.

Replication ensemble - We consider a system containing one polymer template sequence T of length L in contact with four reservoirs: a pool of monomers of m different types M_i with $i = 1 \dots m$ ($m = 4$ for DNA and RNA),

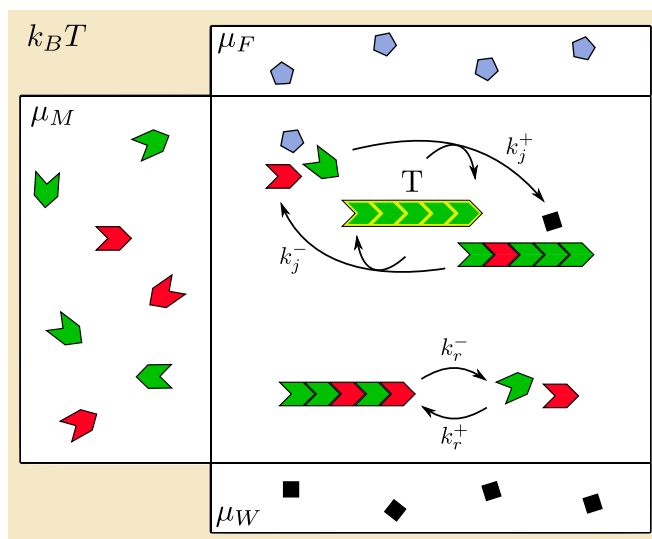
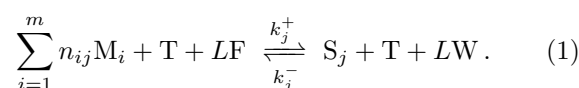


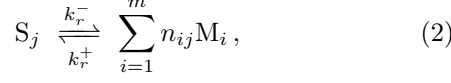
Figure 1. Schematic of the replication ensemble with two monomer types ($m = 2$): green and red. In this example, the template T is composed of green monomers, thus red monomers in sequences S_j are incorrectly copied.

a bath of fuel molecules F , a bath of waste molecules W , and a heat bath at constant temperature (we measure energy in units of the thermal energy, $k_B T = 1$). We call the setting the replication ensemble. Sequences S_j with $j = 1 \dots m^L$ can be generated by copying the template sequence in a process we refer to as templated assembly. Sequences can also be generated by the spontaneous assembly of monomers. The templated copy process consumes fuel F and generates waste W , to produce copy sequences S_j of the same length as the template without altering the template:



Here n_{ij} is a stoichiometric coefficient describing the number of monomers of type i in sequence S_j , with $\sum_{i=1}^m n_{ij} = L$. The templated assembly leading to se-

quence S_j occurs at a rate k_j^+ . Copies are error free if $k_j^+ = 0$ for all sequences j that differ from the template, $S_j \neq T$. Copying errors are captured by finite rates $k_j^+ > 0$ for these sequences. Microscopic reversibility implies that for each j the reverse pathway also exists with rate k_j^- . However, one may expect spontaneous disassembly at rate k_r^- to be more frequent:



with k_r^+ denoting a spontaneous assembly rate.

Microreversibility requires that the templated assembly and disassembly rates obey $k_j^+/k_j^- = e^{-(\Delta\mu_r - \Delta\mu_F)L}$, where $\Delta\mu_r = \epsilon_S/L - \mu_M$ is the per-monomer energy associated with the assembly of a single polymer, and $\Delta\mu_F = \mu_F - \mu_W > 0$ is the per-monomer Gibbs free energy provided by the fuel. Because $\Delta\mu_r$ is independent of the template, its dependence on sequence S_j cannot be used to generate accurate copies of the template [12]. The template behaves as a catalyst and kinetic rates and energy barriers depend on template sequence. We therefore choose $\Delta\mu_r$ to be independent of sequence S_j . We write the rates as $k_j^+ = k_j e^{-(\Delta\mu_r - \Delta\mu_F)L}$, and for the reverse rate $k_j^- = k_j$. Sequence dependence of the process enters via the kinetic coefficients k_j according to $k_j = k_0 e^{-aq}$ [19], where $q \leq L$ is the number of incorrectly copied monomers (the Hamming distance between T and S_j), k_0 is a rate prefactor, and a a specificity.

The spontaneous disassembly and assembly rates also obey $k_r^+/k_r^- = e^{-\Delta\mu_r L}$. We write for the rate of spontaneous assembly $k_r^+ = k_r e^{-\Delta\mu_r L}$ and for the rate of spontaneous disassembly $k_r^- = k_r$, with a sequence-independent coefficient k_r . Note that for now the forward rates k_j^+ and k_r^+ depend on energetics but the backward rates k_j^- and k_r^- do not. In a later section we will relax this assumption.

A schematic representation of the system and reservoirs is provided in fig. 1. Our coarse-grained model describes copying as a one-step process. Polymers of length different from L could occur as intermediate states but are not considered at the coarse-grained level.

Statistics of copying errors - We next determine the probability distribution $p(N_S, t)$ to have N_S copies of sequence S at time t which obeys

$$\partial_t p(N_S, t) = k_a p(N_S - 1, t) - (k_a + N_S k_d) p(N_S, t) + (N_S + 1) k_d p(N_S + 1, t) \quad (3)$$

$$\partial_t p(0, t) = -k_a p(0, t) + k_d p(1, t) \quad (4)$$

with the total assembly rate $k_a = k_j^+ + k_r^+$ and the total disassembly rate $k_d = k_j^- + k_r^-$. We choose as initial condition $P(N_S, 0) = \delta_{N_S}$, yielding a Poisson distribution $p(N_S, t) = \lambda_q^{N_S} e^{-\lambda_q} / N_S!$ for all times, with $\lambda_q = k_a / k_d (1 - \exp(-k_d t))$ [19]. The expected number

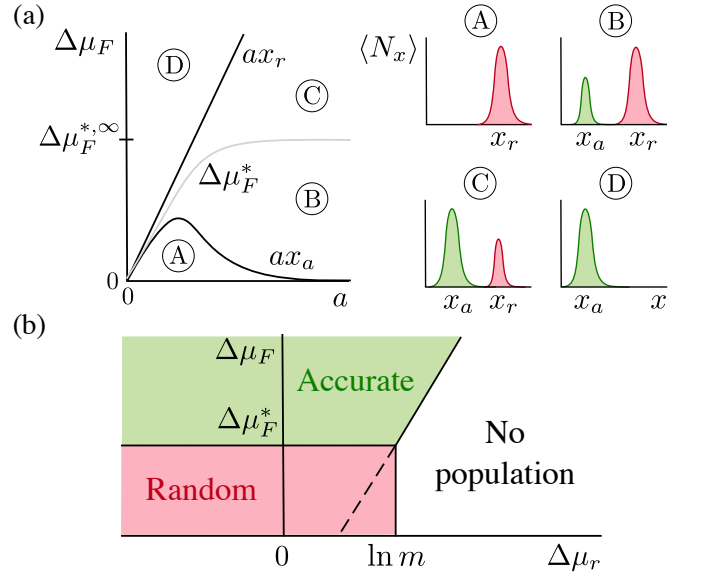


Figure 2. Phase diagrams for (a) finite L and (b) large L with a fixed value of specificity a . (a) $\Delta\mu_F^*, \infty = \ln m + O(L^{-1})$ is the asymptotic value of $\Delta\mu_F^*$ for large specificity a .

of copies $\langle N_x \rangle$ with a monomer error fraction $x = q/L$ is $\langle N_x \rangle = \lambda_{xL} \Omega_{xL}$ with $\Omega_q = \binom{L}{q} (m-1)^q$ the number of sequences with q wrong monomers. For sufficiently long polymers $L \gg 1$, $\langle N_x \rangle$ is dominated by either random copies with error fraction x_r or by accurate copies with error fraction x_a , or both (see fig. 2a). The average fraction of copying errors $\bar{x} = \sum_x x \langle N_x \rangle / \sum_x \langle N_x \rangle$ is used as a measure of copying accuracy. At first order in $1/L$, the error frequencies x_i with $i \in \{r, a\}$ are given by $x_i = x_i^{(0)} - (1 - 2x_i^{(0)}) / (2L) + o(L^{-1})$ with

$$x_r^{(0)} = \frac{m-1}{m} \quad (5)$$

$$x_a^{(0)} = \frac{1}{1 + e^a / (m-1)}. \quad (6)$$

When $a \rightarrow 0$ the templated copying process becomes non-specific and $x_a^{(0)} \rightarrow x_r^{(0)}$. When $a \rightarrow +\infty$ the templated copying process becomes precise and $x_a^{(0)} \rightarrow 0$.

The distribution of copying errors $\langle N_x \rangle$ depends on the Gibbs free energy provided by the fuel $\Delta\mu_F$. We next consider the copying errors in steady-state. If $\Delta\mu_F \leq ax_a$ the number of accurate copies is small, and random sequences dominate. If $\Delta\mu_F \geq ax_r$, the number of random copies is small, and the templated copying process dominates. Under both conditions $\langle N_x \rangle$ is unimodal with a maximum at $x = x_r$ and $x = x_a$, respectively. If instead $ax_a < \Delta\mu_F < ax_r$, random and accurate copies co-exist, and $\langle N_x \rangle$ is bimodal. In this regime, the number of random copies $\langle N_{x_r} \rangle$ and the number of accurate

copies $\langle N_{x_a} \rangle$ are equal when $\Delta\mu_F = \Delta\mu_F^*$, with

$$\Delta\mu_F^* = \ln \left(\frac{m}{1 + (m-1)e^{-a}} \right) + \frac{1}{L} \ln \left(\frac{k_r}{k_0} \sqrt{\frac{x_a^{(0)}(1-x_a^{(0)})}{x_r^{(0)}(1-x_r^{(0)})}} \right) + o\left(\frac{1}{L}\right). \quad (7)$$

These cases are represented in fig. 2a. The dependence of $\Delta\mu_F^*$ on specificity a is shown in fig. 2a in grey.

Phase transition - When increasing $\Delta\mu_F$, we observe a smooth transition of the average error fraction \bar{x} from random copies with error fraction x_r (regions A and B) to accurate copies with error fraction x_a (regions C and D). Since the difference between $\langle N_{x_a} \rangle$ and $\langle N_{x_r} \rangle$ grows exponentially with L in regions B and C, this transition becomes sharp at $\Delta\mu_F = \Delta\mu_F^*$ when $L \rightarrow \infty$, as illustrated in fig. 3a. Therefore, for large L , accurate copies dominate and the average error fraction becomes x_a when $\Delta\mu_F > \Delta\mu_F^*$ where $\Delta\mu_F^*$ depends on specificity a and number of monomer types m . For any value of the specificity, accurate copies dominate in the large L limit when

$$\Delta\mu_F \geq \ln m. \quad (8)$$

This condition can be interpreted as a Landauer's principle [20, 21] for polymer replication: to copy information accurately, the per-monomer externally-provided free energy must be larger than the per-monomer entropy of configuration of the polymer $\ln(m^L)/L$. We refer to $\Delta\mu_F = \ln m$ as the Landauer limit.

Below the Landauer limit ($\Delta\mu_F < \ln m$) the average error fraction \bar{x} decreases as specificity a is increased at low specificity. If specificity a crosses from below a threshold a^* which depends on $\Delta\mu_F$ according to eq. (7), \bar{x} jumps to the value x_r . For finite L , the transition becomes smooth (see fig. 3b). This transition occurs because increasing the specificity a reduces the error fraction x_a associated with accurate copies, but also slows down the overall kinetics of the templated copy process. Because the kinetics of the spontaneous process is independent of a , random copies will eventually dominate. Above the Landauer limit ($\Delta\mu_F \geq \ln m$) the average error fraction \bar{x} decreases as specificity a is increased, but remains accurate and does not undergo a transition towards random copies.

In the large L limit, the transition from random to accurate copies is a first order phase transition. The grey line shown in fig. 2a becomes a first order phase transition line in the limit of large L .

Population size - We next ask if the number of copies that participate in this phase transition can vanish in the large L limit. The number of accurate and random copies, $\langle N_{x_a} \rangle$ and $\langle N_{x_r} \rangle$, depend on the competition between the energetic and entropic contributions: $\ln \langle N_x \rangle / L = \ln \lambda_{xL} / L + \ln \Omega_{xL} / L$. If $\Delta\mu_r > \ln m$, the

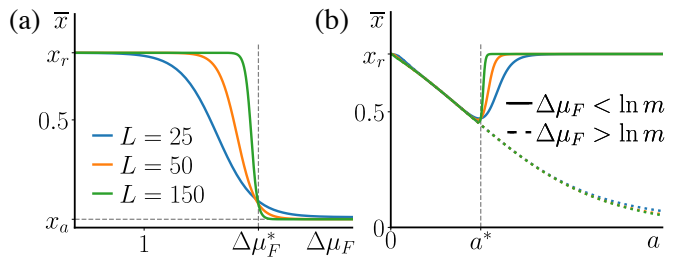


Figure 3. Average error fraction \bar{x} vs (a) energy drive $\Delta\mu_F$ and (b) specificity a , for different values of the template length L (colors apply to (a) and (b)). (a,b) $m = 4$, $k_0 = 1$, $k_r = 0.1$ and $\Delta\mu_r = 0.5$. (a) $a = 3$. (b) $\Delta\mu_F = 2 > \ln 4$ (dotted lines), $\Delta\mu_F = 0.8 < \ln 4$ (plain lines).

population of random copies $\langle N_{x_r} \rangle$ goes extinct for large L , with the energy difference $\ln \lambda_{x_r L} / L = -\Delta\mu_r$ and the entropy of configuration $\ln \Omega_{x_r L} / L = \ln m$. Similarly, if $\Delta\mu_F < \Delta\mu_r - \ln(1 + (m-1)e^{-a})$, the population of accurate copies $\langle N_{x_a} \rangle$ vanishes, with $\ln \lambda_{x_a L} / L = -(\Delta\mu_r - \Delta\mu_F) - ax_a$ and $\ln \Omega_{x_a L} / L = \ln(1 + (m-1)e^{-a}) + ax_a$ [19].

We can now draw a phase diagram in the large L limit as a function of $\Delta\mu_F$ and $\Delta\mu_r$, for a given specificity a , see fig. 2b. This diagram contains three regions: a region where accurate copies dominate, a region where random copies dominate, and a region where the population vanishes. The two boundary lines of the region of vanishing population are given by the two conditions of extinction discussed above. The boundary line between random and accurate copies occurs at $\Delta\mu_F = \Delta\mu_F^*$ where $\Delta\mu_F^* = \ln(m/(1 + (m-1)e^{-a}))$ in the large L limit. The three regions meet at a triple point ($\Delta\mu_r = \ln m$, $\Delta\mu_F = \Delta\mu_F^*$).

Non equilibrium current - We now investigate the non-equilibrium nature of the phase diagrams discussed above. In steady state, total assembly and disassembly are balanced for any sequence S : $k_a = k_d \langle N_S \rangle$. However the templated and spontaneous processes are not balanced individually, which is associated with a non-zero net average fuel current from the fuel bath to the waste bath $\langle J \rangle = L \sum_{j=1}^{m^L} (k_j^+ - \langle N_{S_j} \rangle k_j^-)$. In the large L limit $\langle J \rangle \sim Lk_0 \exp[-(\Delta\mu_r - \Delta\mu_F - \ln(1 + (m-1)e^{-a}))L]$ [19], where \sim describes asymptotic equality in the large L limit.

We now distinguish three regions of the phase diagram which differ in the transduction of fuel energy into useful information. When $\Delta\mu_F < \Delta\mu_r - \ln(1 + (m-1)e^{-a})$, the fuel current vanishes in the large L limit. This region is delimited by the tilted line (both dashed and solid) in fig. 2b. In this case, no fuel is consumed and no accurate copies are produced. The other two regions are located above this tilted line, where the non-vanishing fuel current maintains the system in a non-equilibrium steady-state, and are delimited by the hori-

horizontal line in fig. 2b. If $\Delta\mu_F > \ln(m/(1+(m-1)e^{-a}))$, accurate copies dominate so fuel energy is efficiently converted into information, with $\langle J \rangle \sim Lk_r \langle N_{x_a} \rangle$. If $\Delta\mu_F < \ln(m/(1+(m-1)e^{-a}))$, random copies dominate in the large L limit. In this case, fuel is burnt but no useful information is transmitted.

Kinetic proofreading - Fuel-driven error-correction mechanisms could increase copying accuracy by modifying the kinetics. For example, kinetic proofreading feeds on fuel energy to undo copy errors at the expense of slowing the replication process [18, 22, 23]. In our description of template copying, assembly and disassembly kinetics depend on sequence but energy differences $\Delta\mu_r$ and $\Delta\mu_F$ do not. Hence fuel-driven error-correction mechanisms are in principle implicitly accounted for in our model.

Within our framework, kinetic proofreading can be made explicit as follows. Increasing the specificity a decreases both the error fraction x_a of accurate copies and the templated assembly rates k_j^+ . This increase of the specificity a requires extra fuel energy $\mu_P = \rho\Delta\mu_F$, where ρ denotes the relative cost of proofreading compared to replication. The specificity then becomes a function $a(\mu_P)$. We thus rewrite eq. (1) to explicitly account for kinetic proofreading:

$$\sum_{i=1}^m n_{ij} M_i + T + (1+\rho)LF \xrightleftharpoons[k_j^-]{k_j^+} S_j + T + (1+\rho)LW \quad (9)$$

where we choose $k_j^+ = k_j e^{-(\Delta\mu_r - \Delta\mu_F)L}$, $k_j^- = k_j e^{-\mu_P L}$ and $k_j = k_0 e^{-a(\mu_P)q}$.

In the absence of proofreading, the specificity reduces to the intrinsic specificity $a(\mu_P = 0) \equiv a_0$ of the replication process (eq. (1)). Kinetic proofreading as introduced by Hopfield [22] results in a squared error fraction $x_a(\mu_P) = x_a^2(0)$. We obtain this case if $a(\mu_P) = a_0 + \ln(2 + e^{a_0}/(m-1))$. In the limit of small error rates and thus large specificity, squared error fraction is achieved by doubling the specificity and providing an entropic correction, with $a \sim 2a_0 - \ln(m-1)$.

Implementing kinetic proofreading shifts the boundaries ax_r , $\Delta\mu_F^*$ and ax_a of the phase diagram (fig. 2a), since these depend on a . For sufficiently large specificity a (when $e^a(a-1) > m-1$), the extent of the coexistence regions B and C along the $\Delta\mu_F$ direction will always be enlarged. This implies that it is energetically less costly (smaller $\Delta\mu_F$) to be in a region where accurate copies are made, but it becomes energetically more costly (larger $\Delta\mu_F$) to enter a region where only accurate copies occur.

Generalized reaction rates - So far, the forward rates k_j^+ and k_r^+ depended on energetics but the backward rates k_j^- and k_r^- did not. In this case the rate of templated disassembly $k_j^- = k_0 e^{-axL}$ vanishes for large L while spontaneous disassembly is constant $k_r^- = k_r$. Hence, disassembly in the large L limit is dominated by the spontaneous process. We next discuss a more general

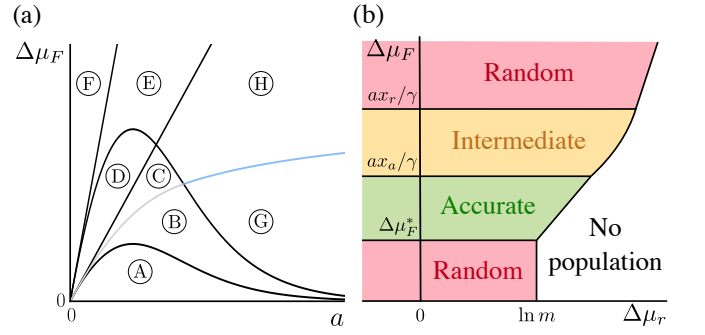


Figure 4. Phase diagrams for the generalized reaction rates eqs. (10) and (11) with $\alpha = \beta$ and $\gamma > 0$, for (a) finite L and (b) large L with a fixed value of a such that $\ln(m/(1+(m-1)e^{-a}))/ (1+\gamma) < ax_a/\gamma$.

parametrization of the kinetic rates for which templated disassembly can compete with spontaneous disassembly. We introduce coefficients $\alpha, \beta, \gamma \in \mathbb{R}$ that allow the disassembly rates to depend on energy differences:

$$k_j^- = k_j e^{-(\alpha\Delta\mu_r - \gamma\Delta\mu_F)L} \quad (10)$$

$$k_r^- = k_r e^{-\beta\Delta\mu_r L}. \quad (11)$$

The assembly rates k_j^+ and k_r^+ also depend on α, β, γ , as imposed by micro-reversibility: $k_j^+/k_j^- = e^{-(\Delta\mu_r - \Delta\mu_F)L}$ and $k_r^+/k_r^- = e^{-\Delta\mu_r L}$. For $\alpha = \beta = \gamma = 0$, we recover the case discussed in the previous sections.

The phase diagram of copying accuracy regimes for general α, β , and γ is shown in [19]. In the following we focus on the special case $\alpha = \beta$, where the energy difference $\Delta\mu_r$ between monomers and polymer has the same effect on the assembly rates of the templated and the spontaneous processes, such that the energy barriers in each case have the same L dependence. Varying the parameter γ for fixed $\alpha = \beta$ changes the ratio of the time-scales associated with the templated and the spontaneous process in an L dependent manner. A positive γ speeds up the kinetics of the templated process compared to $\gamma = 0$, and allows templated disassembly to dominate over spontaneous disassembly for a range of error fractions x . This results in a phase diagram shown in fig. 4a, which exhibits the same four regions A to D shown in fig. 2a and contains four new regions E to H shown in fig. 2a and contains four new regions E to H. Compared to the phase diagram for $\alpha = \beta = \gamma = 0$ shown in fig. 2a, the boundaries of regions A to D are scaled by a factor $1 + \gamma$, but the statistics of error fractions in these regions remain the same. In the new region E the distribution of copying errors in the large L limit is unimodal with a single peak at error fraction $x_m = \gamma\Delta\mu_F/a$. Region E is separated from region F by $\Delta\mu_F = ax_r/\gamma$, from region H by $\Delta\mu_F = ax_r/(1+\gamma)$, and from region D by $\Delta\mu_F = ax_a/\gamma$. As $\Delta\mu_F$ is increased, x_m increases linearly from x_a at the boundary between regions D and E to x_r at the boundary between

regions E and F. We thus call x_m the intermediate error fraction. In region F, where $\Delta\mu_F > ax_r/\gamma$, assembly and disassembly are both governed by the templated process for error fractions $x \leq x_r$. Since disassembly is now also sequence-dependent, accurate copies are disassembled faster than inaccurate ones, and the steady-state generated by the templated process becomes sequence-independent with dominating error fraction x_r . Regions G and H are regions of phase coexistence between random copies with error fraction x_r and copies with intermediate error fraction x_m . These regions are separated from region E by $\Delta\mu_F = ax_r/(1 + \gamma)$ and from regions B and C by $\Delta\mu_F = ax_a/\gamma$. Regions G and H are separated from each other by the non-analytic curve representing the equality between the copy numbers of both phases, shown in light blue in fig. 4a.

We show in fig. 4b the phase diagram in the large L limit for a fixed value of specificity a such that $\ln(m/(1 + (m - 1)e^{-a}))/ (1 + \gamma) < ax_a/\gamma$. Similar to the example shown in fig. 2b, for small $\Delta\mu_F$, the system generates random copies. The transition from random to accurate copies occurs at the threshold $\Delta\mu_F^*$, which is reduced by a factor $1 + \gamma$ relative to the value given in eq. (7) [19]. Further increasing $\Delta\mu_F$ leads to a continuous increase in the average error fraction until the system re-enters a regime of random copying. There is thus a range of values $\Delta\mu_F^* < \Delta\mu_F < ax_a/\gamma$ where a maximum accuracy at error fraction x_a is achieved. In the large L , the number of copies can vanish, which is indicated by the white region in fig. 4b. Extinction conditions are given explicitly in [19].

Discussion - In this Letter we study populations of copolymer copies and their accuracy in a thermodynamically consistent replication ensemble. We find sharp transitions between populations of random and accurate copies as a function of fuel driving and copying specificity. Our coarse-grained approach reveals generic features of stochastic copying processes that are independent of many molecular details. It allows for an evaluation of the role of fuel driving, proofreading, and energy barriers on the population of accurate copies. We identify for given specificity the minimal cost of Gibbs free energy $\Delta\mu_F^*$ required to maintain a population of accurate copies. The minimal Gibbs free energy cost to be in a regime of accurate copying regardless of the specificity is given by the per monomer configurational entropy. In analogy to the Landauer principle of information erasure we refer to this as the Landauer limit.

It will be interesting to extend this framework to allow the copies of the template polymer to be themselves replicated, perhaps offering new means to investigate the link between the statistical mechanics of replicating systems and the evolutionary process [24–27]. This might also allow for a re-investigation of Eigen’s paradox of achieving high fidelity copies of large genomes [28, 29]. More generally, other problems associated with the origin-of-

life question could perhaps be freshly investigated within the replication ensemble [30–36].

While inspired by the copy process of biological DNA polymers [19], our formalism more generally applies to systems of information transfer from a template to a copy of the template. For example, our approach equally applies to the copy process from RNA to protein (translation, with 20 ‘monomer’ types), or more generally for copy processes with any number of monomer types. Our formalism allows for the discussion of a trade-off that arises when increasing the number m of monomer types, for large L . The energetic cost required to be in a regime of accurate copying is high for low values of m as compared to large values of m , but the accuracy of copies is higher. This is because an increase of m allows for the use of shorter polymers for encoding the same amount of information, while the more complex encoding is more prone to mistakes (eq. (6)). Indeed, the minimal energy to copy a sequence with information content $\Omega = m^L$ with accuracy a is given by $E_{\text{tot}}^* = L(m)\Delta\mu_F^* = (1 - \ln(1 + (m - 1)e^{-a}) / \ln m) \ln \Omega$, which decreases with m . It is interesting to speculate that this cost-accuracy trade-off is relevant from an evolutionary point of view, manifested in the choice of $m = 4$ for maintaining the genome in DNA form at high fidelity, and for copying genomic information to protein peptide sequences with $m = 20$ at lower energetic costs and reduced requirements on fidelity.

-
- [1] A. Kornberg and T. A. Baker, *DNA Replication*, 2nd ed. (W. H. Freeman and Company, New York, 1992).
 - [2] I. Lieberman, A. Kornberg, and E. S. Simms, Enzymatic synthesis of nucleoside diphosphates and triphosphates, *J. Biol. Chem.* **215**, 429 (1955).
 - [3] G. T. Yarranton and M. L. Gefter, Enzyme-catalyzed DNA unwinding: Studies on *Escherichia coli* *rep* protein, *Proc. Natl. Acad. Sci. U.S.A.* **76**, 1658 (1979).
 - [4] I. Lehman, M. J. Bessman, E. S. Simms, and A. Kornberg, Enzymatic Synthesis of Deoxyribonucleic Acid, *J. Biol. Chem.* **233**, 163 (1958).
 - [5] W. Yang, Nucleases: diversity of structure, function and mechanism, *Quart. Rev. Biophys.* **44**, 1 (2011).
 - [6] D. Andrieux and P. Gaspard, Nonequilibrium generation of information in copolymerization processes, *Proc. Natl. Acad. Sci. U.S.A.* **105**, 9516 (2008).
 - [7] D. Andrieux and P. Gaspard, Molecular information processing in nonequilibrium copolymerizations, *J. Chem. Phys.* **130**, 014901 (2009).
 - [8] P. Sartori and S. Pigolotti, Kinetic versus Energetic Discrimination in Biological Copying, *Phys. Rev. Lett.* **110**, 188101 (2013).
 - [9] P. Gaspard and D. Andrieux, Kinetics and thermodynamics of first-order Markov chain copolymerization, *J. Chem. Phys.* **141**, 044908 (2014).
 - [10] P. Sartori and S. Pigolotti, Thermodynamics of Error Correction, *Phys. Rev. X* **5**, 041039 (2015).

- [11] R. Rao and L. Peliti, Thermodynamics of accuracy in kinetic proofreading: dissipation and efficiency trade-offs, *J. Stat. Mech.* **2015**, P06001 (2015).
- [12] T. E. Ouldridge and P. Rein ten Wolde, Fundamental Costs in the Production and Destruction of Persistent Polymer Copies, *Phys. Rev. Lett.* **118**, 158103 (2017).
- [13] J. M. Poulton, P. Rein ten Wolde, and T. E. Ouldridge, Nonequilibrium correlations in minimal dynamical models of polymer copying, *Proc. Natl. Acad. Sci. U.S.A.* **116**, 1946 (2019).
- [14] D. Chiuchiú, Y. Tu, and S. Pigolotti, Error-Speed Correlations in Biopolymer Synthesis, *Phys. Rev. Lett.* **123**, 038101 (2019).
- [15] M. Sahoo, A. Noushad, P. R. Baral, and S. Klumpp, Accuracy and speed of elongation in a minimal model of DNA replication, *Phys. Rev. E* **104**, 034417 (2021).
- [16] J. M. Poulton and T. E. Ouldridge, Edge-effects dominate copying thermodynamics for finite-length molecular oligomers, *New J. Phys.* **23**, 063061 (2021).
- [17] J. Juritz, J. M. Poulton, and T. E. Ouldridge, Minimal mechanism for cyclic templating of length-controlled copolymers under isothermal conditions, *J. Chem. Phys.* **156**, 074103 (2022).
- [18] C. H. Bennett, Dissipation-error tradeoff in proofreading, *Biosystems* **11**, 85 (1979).
- [19] See Supplemental Material at [URL will be inserted by publisher] for mathematical derivations.
- [20] R. Landauer, Irreversibility and Heat Generation in the Computing Process, *IBM J. Res. Dev.* **5**, 183 (1961).
- [21] D. Andrieux and P. Gaspard, Information erasure in copolymers, *EPL* **103**, 30004 (2013).
- [22] J. J. Hopfield, Kinetic Proofreading: A New Mechanism for Reducing Errors in Biosynthetic Processes Requiring High Specificity, *Proc. Natl. Acad. Sci. U.S.A.* **71**, 4135 (1974).
- [23] M. Depken, J. M. Parrondo, and S. W. Grill, Intermittent Transcription Dynamics for the Rapid Production of Long Transcripts of High Fidelity, *Cell Rep.* **5**, 521 (2013).
- [24] N. Goldenfeld and C. Woese, Life is physics: Evolution as a collective phenomenon far from equilibrium, *Annu. Rev. Condens. Matter Phys.* **2**, 375 (2011).
- [25] L. A. Demetrius, Boltzmann, Darwin and Directionality theory, *Phys. Rep.* **530**, 1 (2013).
- [26] J. L. England, Statistical physics of self-replication, *J. Chem. Phys.* **139**, 121923 (2013).
- [27] A. Genthon, R. García-García, and D. Lacoste, Branching processes with resetting as a model for cell division, *J. Phys. A: Math. Theor.* **55**, 074001 (2022).
- [28] M. Eigen, Selforganization of matter and the evolution of biological macromolecules, *Naturwissenschaften* **58**, 465 (1971).
- [29] I. Leuthäusser, Statistical mechanics of Eigen's evolution model, *J. Stat. Phys.* **48**, 343 (1987).
- [30] A. V. Tkachenko and S. Maslov, Spontaneous emergence of autocatalytic information-coding polymers, *J. Chem. Phys.* **143**, 045102 (2015).
- [31] Y. J. Matsubara and K. Kaneko, Optimal size for emergence of self-replicating polymer system, *Phys. Rev. E* **93**, 032503 (2016).
- [32] Y. J. Matsubara and K. Kaneko, Kinetic Selection of Template Polymer with Complex Sequences, *Phys. Rev. Lett.* **121**, 118101 (2018).
- [33] A. V. Tkachenko and S. Maslov, Onset of natural selection in populations of autocatalytic heteropolymers, *J. Chem. Phys.* **149**, 134901 (2018).
- [34] J. H. Rosenberger, T. Göppel, P. W. Kudella, D. Braun, U. Gerland, and B. Altaner, Self-Assembly of Informational Polymers by Templated Ligation, *Phys. Rev. X* **11**, 031055 (2021).
- [35] P. W. Kudella, A. V. Tkachenko, A. Salditt, S. Maslov, and D. Braun, Structured sequences emerge from random pool when replicated by templated ligation, *Proc. Natl. Acad. Sci. U.S.A.* **118**, e2018830118 (2021).
- [36] T. Göppel, J. H. Rosenberger, B. Altaner, and U. Gerland, Thermodynamic and Kinetic Sequence Selection in Enzyme-Free Polymer Self-Assembly inside a Non-equilibrium RNA Reactor, *Life* **12**, 567 (2022).

Supplemental Information for ‘Non Equilibrium Transitions in a Polymer Replication Ensemble’

Arthur Genthon, Carl D. Modes, Frank Jülicher, and Stephan W. Grill

I. STATISTICS OF ERRORS

A. Solving the master equation

We recast the master equation (eq. 3 in the main text) as an partial differential equation for the generating function

$$G(z, t) = \sum_{N=0}^{\infty} z^N p(N, t) \quad (\text{S1})$$

by multiplying it by z^N and summing over N :

$$\partial_t G(z, t) = -k_d(z-1)\partial_z G(z, t) + k_a(z-1)G(z, t). \quad (\text{S2})$$

This equation is solved with the method of characteristics by choosing the parametrization $\hat{G}(x) = G(z(x), t(x))$ with $t(x) = x$ and $dz/dx = k_d(z-1)$ such that the ordinary differential equation

$$\frac{d\hat{G}}{dx} = k_a(z(x)-1)\hat{G}(x) \quad (\text{S3})$$

is solvable and gives the solution

$$\hat{G}(x) = \hat{G}(0) \exp \left[\int_0^x k_a(z(x')-1) dx' \right], \quad (\text{S4})$$

where $\hat{G}(0) = G(z(0), 0) \equiv G_0(z(0))$ is the initial condition.

Integrating dz/dx gives $z(x) = (z(0)-1)\exp(k_d x) + 1$, so that the solution reads:

$$G(z, t) = G_0 \left(1 + (z-1)e^{-k_d t} \right) e^{(z-1)\lambda(t)} \quad (\text{S5})$$

$$\lambda(t) = \frac{k_a}{k_d} \left(1 - e^{-k_d t} \right). \quad (\text{S6})$$

We start at time $t = 0$ with no copy sequences in our system, $p(N, t=0) = \delta_N$, which implies $G_0 = 1$. Finally, the solution is a Poisson distribution at all times, with rate $\lambda(t)$:

$$p(N, t) = \frac{\lambda(t)^N}{N!} e^{-\lambda(t)}. \quad (\text{S7})$$

For any length L , k_d is finite and the solution converges towards the steady-state Poisson distribution with rate k_a/k_d .

B. Distribution for the number of copies with q errors

We now derive the distribution $Q(N_q, t)$ for the number N_q of polymers with q errors when compared to the template at time t . There are $\Omega_q = \binom{L}{q} (m-1)^q$ sequences with q errors, which we label $1 \leq i_1 < \dots < i_{\Omega_q} \leq m^L$, associated with numbers of copies $N_{i_1}, \dots, N_{i_{\Omega_q}}$. The distribution thus reads:

$$Q(N_q, t) = \sum_{N_{i_1} + \dots + N_{i_{\Omega_q}} = N_q} p(N_{i_1}, \dots, N_{i_{\Omega_q}}, t). \quad (\text{S8})$$

Since sequences are independent, the joint distribution of copy numbers is the product of the marginal distributions given by eq. (S7), which share the same rate $\lambda_q(t)$. Therefore, using the multinomial theorem, we get that the distribution Q is also Poissonian with rate $\lambda_q(t)\Omega_q$:

$$Q(N_q, t) = \lambda_q(t)^{N_q} e^{-\lambda_q(t)\Omega_q} \sum_{N_{i_1} + \dots + N_{i_{\Omega_q}} = N_q} \prod_{j=1}^{\Omega_q} (N_{i_j}!)^{-1} \quad (\text{S9})$$

$$= \frac{(\lambda_q(t)\Omega_q)^{N_q}}{N_q!} e^{-\lambda_q(t)\Omega_q}. \quad (\text{S10})$$

Finally, the average number of polymers with error fraction $x = q/L$ is equal to

$$\langle N_x(t) \rangle = \lambda_{xL}(t)\Omega_{xL}. \quad (\text{S11})$$

II. PHASE DIAGRAM

We now investigate which sequences are dominant in the steady-state population in the large L limit. To do so, we define the monomer error fraction, $x = q/L$, and seek the maxima of the expected number $\langle N_x \rangle = \lambda_{xL}\Omega_{xL}$ of sequences with an error fraction x . We treat here the most general case defined by eqs. (10-11) in the main text.

Since $\langle N_x \rangle$ grows exponentially with L , it is convenient to instead work with

$$f(x) = -\frac{1}{L} \ln \langle N_x \rangle \quad (\text{S12})$$

$$= -\frac{1}{L} \ln \left[\binom{L}{xL} (m-1)^{xL} e^{-\Delta\mu_r L} \frac{k_0 e^{(-ax - \alpha\Delta\mu_r + (1+\gamma)\Delta\mu_F)L} + k_r e^{-\beta\Delta\mu_r L}}{k_0 e^{(-ax - \alpha\Delta\mu_r + \gamma\Delta\mu_F)L} + k_r e^{-\beta\Delta\mu_r L}} \right] \quad (\text{S13})$$

We use Stirling formula, $n! = \sqrt{2\pi n}(n/e)^n(1 + O(1/n))$ for large n :

$$\binom{L}{xL} = (2\pi Lx(1-x))^{-1/2} x^{-xL} (1-x)^{-(1-x)L} \left(1 + O\left(\frac{1}{L}\right)\right). \quad (\text{S14})$$

We simplify the denominator and numerator of the fraction as

$$\begin{aligned} \frac{1}{L} \ln \left(k_0 e^{(-ax - \alpha\Delta\mu_r + \gamma\Delta\mu_F)L} + k_r e^{-\beta\Delta\mu_r L} \right) &= \left(-ax - \alpha\Delta\mu_r + \gamma\Delta\mu_F + \frac{\ln k_0}{L} \right) \theta(x_m - x) \\ &\quad + \left(-\beta\Delta\mu_r + \frac{\ln k_r}{L} \right) \theta(x - x_m) + o\left(\frac{1}{L}\right) \end{aligned} \quad (\text{S15})$$

$$\begin{aligned} \frac{1}{L} \ln \left(k_0 e^{(-ax - \alpha\Delta\mu_r + (1+\gamma)\Delta\mu_F)L} + k_r e^{-\beta\Delta\mu_r L} \right) &= \left(-ax - \alpha\Delta\mu_r + (1+\gamma)\Delta\mu_F + \frac{\ln k_0}{L} \right) \theta(x_M - x) \\ &\quad + \left(-\beta\Delta\mu_r + \frac{\ln k_r}{L} \right) \theta(x - x_M) + o\left(\frac{1}{L}\right) \end{aligned} \quad (\text{S16})$$

with θ the Heaviside function and the threshold error fractions

$$x_m = \frac{(\beta - \alpha)\Delta\mu_r + \gamma\Delta\mu_F}{a} \quad (\text{S17})$$

$$x_M = \frac{(\beta - \alpha)\Delta\mu_r + (1 + \gamma)\Delta\mu_F}{a}, \quad (\text{S18})$$

which are such that $x_M - x_m = \Delta\mu_F/a > 0$.

Combining these results we obtain

$$f(x) = g(x) + \frac{1}{2L} \ln(2\pi Lx(1-x)) + \Delta\mu_r + \begin{cases} -\Delta\mu_F + o\left(\frac{1}{L}\right) & \text{if } x < x_m \\ ax + (\alpha - \beta)\Delta\mu_r - (1 + \gamma)\Delta\mu_F + \frac{\ln(k_r/k_0)}{L} + o\left(\frac{1}{L}\right) & \text{if } x_m < x < x_M \\ o\left(\frac{1}{L}\right) & \text{if } x_M < x \end{cases} \quad (\text{S19})$$

where we defined the function

$$g(x) = x \ln \left(\frac{x}{m-1} \right) + (1-x) \ln(1-x). \quad (\text{S20})$$

We seek the minima of f at first order in $1/L$:

$$x = x^{(0)} + \frac{x^{(1)}}{L} + o\left(\frac{1}{L}\right). \quad (\text{S21})$$

At zero-th order, the minima of $g(x)$ and of $h(x) = g(x) + ax$ are respectively:

$$x_r^{(0)} = \frac{m-1}{m} \quad (\text{S22})$$

$$x_a^{(0)} = \frac{1}{1 + e^a/(m-1)}, \quad (\text{S23})$$

with $g(x_r^{(0)}) = -\ln m$ and $h(x_r^{(0)}) = -\ln(1 + (m-1)e^{-a})$.

The first order corrections are obtained by injecting $x = x^{(0)} + x^{(1)}/L$ in $f'(x) = 0$, which leads to

$$x^{(1)} = - \left. \frac{(\ln(x(1-x)))'}{2g''(x)} \right|_{x=x^{(0)}} \quad (\text{S24})$$

$$= \frac{2x^{(0)} - 1}{2}, \quad (\text{S25})$$

both for the accurate and random copies, since $g''(x) = (g(x) + ax)''$.

Whether or not these minima x_r and x_a are reached by f depends on their relative positions with the threshold error fractions x_m and x_M . For example, if $x_a \in [x_m, x_M]$, where f is equal to h (+ corrections), then f reaches a local minimum at x_a , while if $x_a \notin [x_m, x_M]$, then f has no local minimum on $[x_m, x_M]$. There are 6 cases (because $x_a < x_r$ and $x_m < x_M$), listed below, and represented on fig. S1 where the dots indicate the minima of f .

1. $x_m < x_M < x_a < x_r$: Global minimum x_r
2. $x_m < x_a < x_M < x_r$: Local minima (x_a, x_r)
3. $x_m < x_a < x_r < x_M$: Global minimum x_a
4. $x_a < x_m < x_r < x_M$: Global minimum x_m
5. $x_a < x_r < x_m < x_M$: Global minimum x_r
6. $x_a < x_m < x_M < x_r$: Local minima (x_m, x_r)

In the end, f has either one or two minima, corresponding to one or two peaks in the population $\langle N_x \rangle$. Note that since x_m is threshold error fraction for the definition of the piece-wise function f , it is a local minimum of f only when f is decreasing on $[0, x_m]$ and increasing on $[x_m, x_M]$, i.e. when $x_a < x_m < x_r$.

In cases 2 and 6, where $\langle N_x \rangle$ is bimodal, the relative height of the two peaks is given by the difference in the values of f at the two error fractions. For example, in case 2 we have

$$f(x_r) = -\ln(m) + \frac{1}{2L} \ln \left(2\pi L x_r^{(0)} (1 - x_r^{(0)}) \right) + \Delta\mu_r + o\left(\frac{1}{L}\right) \quad (\text{S26})$$

$$f(x_a) = -\ln(1 + (m-1)e^{-a}) + \frac{1}{2L} \ln \left(2\pi L x_a^{(0)} (1 - x_a^{(0)}) \right) + (1 + \alpha - \beta)\Delta\mu_r - (1 + \gamma)\Delta\mu_F + \frac{\ln(k_r/k_0)}{L} + o\left(\frac{1}{L}\right). \quad (\text{S27})$$

The two populations are thus equal, $\langle N_{x_r} \rangle = \langle N_{x_a} \rangle$ (peaks of the same height), when $\Delta\mu_F = \Delta\mu_F^*$ with

$$\Delta\mu_F^* = \frac{1}{1 + \gamma} \left[\ln \left(\frac{m}{1 + (m-1)e^{-a}} \right) - (\beta - \alpha)\Delta\mu_r + \frac{1}{L} \ln \left(\frac{k_r}{k_0} \sqrt{\frac{x_a^{(0)}(1 - x_a^{(0)})}{x_r^{(0)}(1 - x_r^{(0)})}} \right) + o\left(\frac{1}{L}\right) \right]. \quad (\text{S28})$$

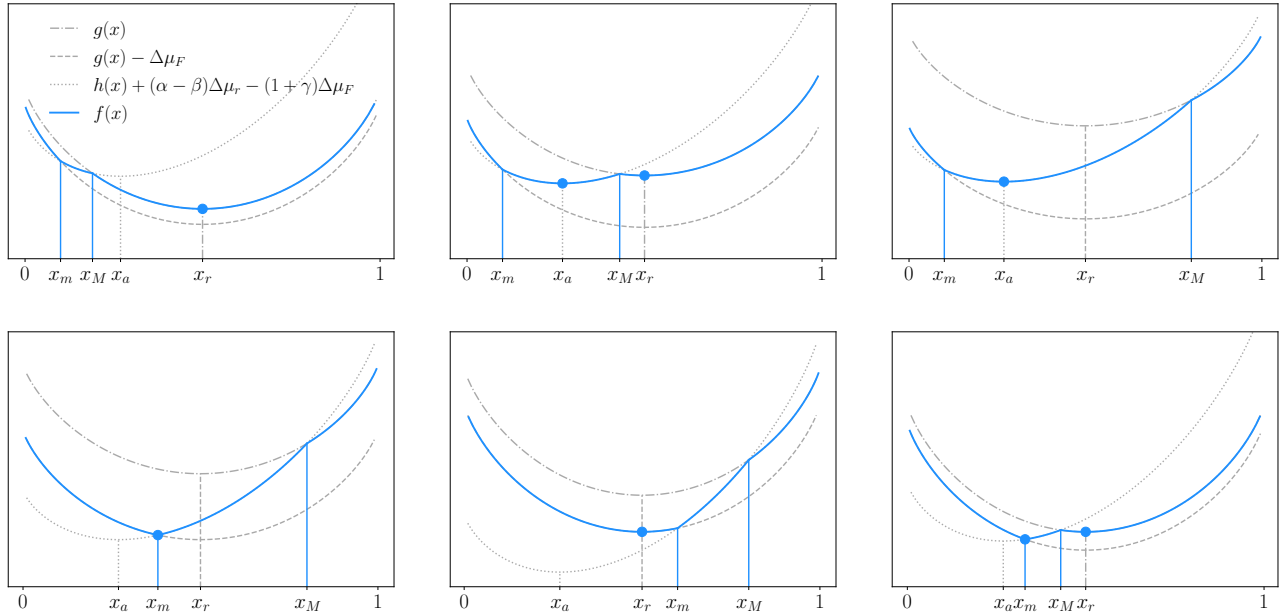


Figure S1. Plots of function $f(x) = -\ln\langle N_x \rangle/L$, shown in blue, versus error fraction x , in the 6 cases defined in the text. The grey dotted, dashed and dash-dotted curves are the three functions that define f in a piece-wise manner in eq. (S19). The minima of function f are indicated with blue circles.

When $\alpha = \beta = \gamma = 0$, this result gives back eq. (7) in the main text.

We show on fig. S2 an example of general phase diagram. The regions A to H correspond to the cases 1 to 6 in the following manner: the regions A, D, E and F of unimodal population $\langle N_x \rangle$ correspond to the cases 1, 3, 4 and 5 respectively. The regions (B,C) and (G,H) of bimodal population $\langle N_x \rangle$ correspond respectively to the two sub-regions of cases 2 and 6, defined by the dominance of one or other of the two error fractions, and are delimited by dotted curves of equal populations. The inequalities between x_m , x_M , x_a and x_r which define the 6 cases give the equations of the phase borders. To plot this phase diagram, we chose $\alpha < \beta$ and $\gamma > 0$, but similar diagrams are obtained for other values of the parameters.

In the main text we treated the case $\alpha = \beta$. In this case, all the phase borders become horizontal, and the regions G and H are not accessible anymore. In the simple case treated at first, when $\alpha = \beta = \gamma = 0$, then $x_m = 0$, and thus the cases 4, 5 and 6 are not possible, and the regions E to H are not accessible.

III. POPULATION SIZE

In this section we investigate the conditions under which the numbers of copies with error fractions x_r , x_a and x_m vanish in the large L limit. Regions of vanishing population are represented in white in Figures 2b and 4b in the main text.

In region A, the average number of copies $\langle N_x \rangle$ is characterized by a single peak around $x = x_r$. This region corresponds to case 1 in section II where $x_M < x_r$, so that in the large L limit eq. (S19) reads

$$f(x_r) = -\ln m + \Delta\mu_r. \quad (\text{S29})$$

The population of random copies therefore goes extinct if $\Delta\mu_r > \ln m$.

In region F, the average number of copies $\langle N_x \rangle$ is also characterized by a single peak around $x = x_r$. This region corresponds to case 5 in section II where $x_r < x_m$, so that in the large L limit eq. (S19) reads

$$f(x_r) = -\ln m + \Delta\mu_r - \Delta\mu_F. \quad (\text{S30})$$

The population of random copies therefore goes extinct if $\Delta\mu_F < \Delta\mu_r - \ln m$. The line separating the phases of no population in white and random copies in red for $\Delta\mu_F > ax_r/\gamma$ in Fig and 4b is thus of slope 1.

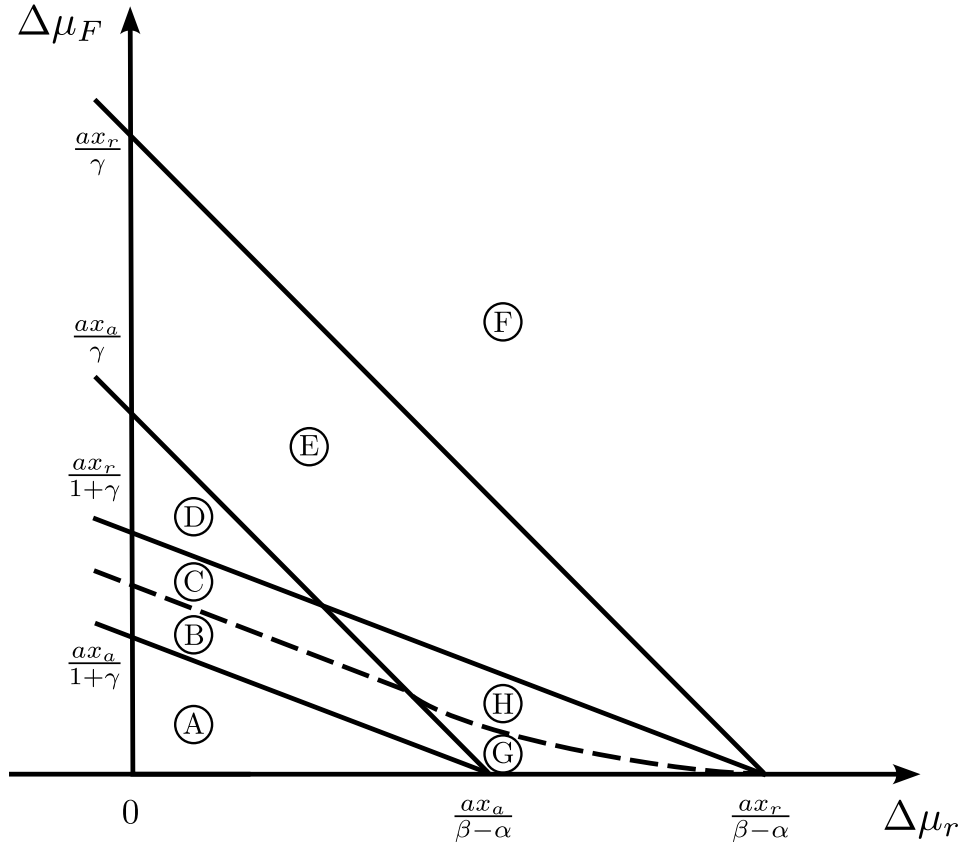


Figure S2. Phase diagram for a fixed value of specificity a , in the case $\alpha < \beta$ and $\gamma > 0$. The regions A to H are characterized by the existence of one or two peaks of the average number of copies $\langle N_x \rangle$ at error fractions specified in the text.

The reason why these two conditions are different even though the accuracy x_r of the copies is the same in regions A and F is because in region A, both assembly and disassembly are controlled by the spontaneous process while in region F, both are controlled by the templated process. In both regions A and F, the steady-state generated by these processes is sequence-independent with dominating error fraction x_r , but the energies involved are different. The fuel burnt in the templated reaction allows for non-vanishing populations of copies for values of $\Delta\mu_r$ larger than $\ln m$.

In region D, the average number of copies $\langle N_x \rangle$ is characterized by a single peak around $x = x_a$. This region corresponds to case 3 in section II where $x_m < x_a < x_M$, so that in the large L limit eq. (S19) reads

$$f(x_a) = -\ln(1 + (m-1)e^{-a}) + (1 + \alpha - \beta)\Delta\mu_r - (1 + \gamma)\Delta\mu_F. \quad (\text{S31})$$

The population of accurate copies therefore goes extinct if $\Delta\mu_F < ((1 + \alpha - \beta)\Delta\mu_r - \ln(1 + (m-1)e^{-a}))/ (1 + \gamma)$. In Fig 4b, plot in the case $\alpha = \beta$ and $\gamma > 0$, the line separating the phases of no population in white and accurate copies in green is thus of slope $1/(1 + \gamma)$, and in Fig 2b, plot in the case $\alpha = \beta = \gamma = 0$, the same line has a slope 1.

In region E, the average number of copies $\langle N_x \rangle$ is characterized by a single peak around $x = x_m$. This region corresponds to case 4 in section II, so that in the large L limit eq. (S19) reads

$$f(x_m) = g(x_m) + \Delta\mu_r - \Delta\mu_F. \quad (\text{S32})$$

The population of intermediate copies therefore goes extinct if $\Delta\mu_F < \Delta\mu_r + g(x_m)$. This condition is non-analytical in $\Delta\mu_F$, and is represented by the curve separating the phases of no population in white and intermediate copies in yellow in Fig 4b. One straightforwardly shows that there is no discontinuity in the derivative between this curve and the straight lines in the neighboring regions of accurate and intermediate copies.

In regions of phase coexistence, B-C and G-H, the conditions for the extinction of the population associated with each error fraction are the same as the ones given above. For example, in regions B and C, the average number of copies $\langle N_x \rangle$ is characterized by two peaks around $x = x_r$ and $x = x_a$. These two regions correspond to case 2 in section II, where $x_m < x_a < x_M < x_r$. Thus, the population of random copies goes extinct if $\Delta\mu_r > \ln m$, like in region A where $x_M < x_r$ as well, and the population of accurate copies goes extinct if $\Delta\mu_F < ((1 + \alpha - \beta)\Delta\mu_r - \ln(1 + (m-1)e^{-a}))/ (1 + \gamma)$ like in region D where $x_m < x_a < x_M$ as well.

IV. NON-EQUILIBRIUM CURRENT

We compute here the net average current of fuel molecules from the fuel bath to the waste bath $\langle J \rangle = L \sum_{j=1}^{m^L} (k_j^+ - \langle N_{S_j} \rangle k_j^-)$, in the case $\alpha = \beta = \gamma = 0$ treated in the first part of the main text. Since disassembly is dominated by the spontaneous process, we expect a negligible amount of fuel molecules released by templated disassembly. Indeed, the average flux associated with a given sequence S_j with error fraction x reads:

$$L(k_j^+ - \langle N_{S_j} \rangle k_j^-) = Lk_0 e^{-(\Delta\mu_r - \Delta\mu_F + ax)L} \left[1 - \frac{k_0 e^{-axL} + k_r e^{-\Delta\mu_F L}}{k_0 e^{-axL} + k_r} \right], \quad (\text{S33})$$

where we replaced $\langle N_{S_j} \rangle$ by its expression $(k_j^+ + k_r^+) / (k_j^- + k_r^-)$. Since the fuel drive $\Delta\mu_F$ and the specificity a are positive, the term in the bracket goes to 1 in the large L limit, so that $L(k_j^+ - \langle N_{S_j} \rangle k_j^-) \sim Lk_j^+$.

The total flux is then given by:

$$\langle J \rangle \sim Lk_0 e^{-(\Delta\mu_r - \Delta\mu_F)L} \sum_{j=1}^{m^L} e^{-aq_j}, \quad (\text{S34})$$

with q_j the number of errors of sequence S_j . The sum is computed as follows

$$\sum_{j=1}^{m^L} e^{-aq_j} = \sum_{q_j=0}^L \Omega_{q_j} e^{-aq_j} \quad (\text{S35})$$

$$= \sum_{q_j=0}^L \binom{L}{q_j} ((m-1)e^{-a})^{q_j} \quad (\text{S36})$$

$$= [1 + (m-1)e^{-a}]^L. \quad (\text{S37})$$

We recover the result from the main text, in the large L limit

$$\langle J \rangle \sim Lk_0 \exp \left[-(\Delta\mu_r - \Delta\mu_F - \ln(1 + (m-1)e^{-a}))L \right]. \quad (\text{S38})$$

V. CHOICE OF KINETIC PREFACTOR FOR THE TEMPLATED REACTION

In our model, the sequence-selectivity of the templated process enters via the kinetic prefactor k_j involved in both the assembly and disassembly rates k_j^+ and k_j^- . In principle, any function k_j of the number q of errors (number of incorrectly copied monomers) is acceptable. However, we show in this section that any choice other than the exponential dependence of k_j on q does not achieve sequence-selection. The reason is that kinetic rates are exponential in length L , since they are exponential in energies which themselves scale with L , and the number of sequences with error fraction x is also exponential in L in the large L limit.

For any function k_j which is super-exponential in $q = xL$, the kinetic rates of templated assembly and disassembly decay too fast, and thus both the assembly and disassembly reactions are dominated by the spontaneous process. The statistics of errors resulting from the spontaneous process alone is governed by combinatorial effects and dominated by random copies. This can be seen by following the derivation of section II but choosing $k_j = k_0 e^{-aq^b}$ with $b > 1$. In this case, in the large L limit, eqs. (S15) and (S16) are modified as follows

$$\frac{1}{L} \ln \left(k_0 e^{-ax^b L^b + (-\alpha\Delta\mu_r + \gamma\Delta\mu_F)L} + k_r e^{-\beta\Delta\mu_r L} \right) = -\beta\Delta\mu_r + o\left(\frac{1}{L}\right) \quad (\text{S39})$$

$$\frac{1}{L} \ln \left(k_0 e^{-ax^b L^b + (-\alpha\Delta\mu_r + (1+\gamma)\Delta\mu_F)L} + k_r e^{-\beta\Delta\mu_r L} \right) = -\beta\Delta\mu_r + o\left(\frac{1}{L}\right), \quad (\text{S40})$$

for all values of α , β and γ . The number of copies with error fraction x is thus given by the function:

$$f(x) = g(x) + \frac{1}{2L} \ln(2\pi Lx(1-x)) + \Delta\mu_r + o\left(\frac{1}{L}\right) \quad (\text{S41})$$

which has a single minimum at error fraction x_r .

For any function k_j which is sub-exponential in $q = xL$, the energetic contributions to k_j^+ and k_j^- control the sequence-selection. Since these energies are sequence-independent in our model, the statistics of errors is governed by combinatorial effects again, and results in an average error fraction x_r . This can be seen by following the derivation of section II but choosing $k_j = k_0 e^{-aq^b}$ with $b < 1$. In this case, in the large L limit, eqs. (S15) and (S16) are modified as follows

$$\begin{aligned} \frac{1}{L} \ln \left(k_0 e^{-ax^b L^b + (-\alpha \Delta\mu_r + \gamma \Delta\mu_F)L} + k_r e^{-\beta \Delta\mu_r L} \right) &= \left(-\alpha \Delta\mu_r + \gamma \Delta\mu_F + \frac{\ln k_0 - ax^b L^b}{L} \right) \theta(\gamma \Delta\mu_F - (\alpha - \beta) \Delta\mu_r) \\ &+ \left(-\beta \Delta\mu_r + \frac{\ln k_r}{L} \right) \theta((\alpha - \beta) \Delta\mu_r - \gamma \Delta\mu_F) + o\left(\frac{1}{L}\right) \end{aligned} \quad (\text{S42})$$

$$\begin{aligned} \frac{1}{L} \ln \left(k_0 e^{-ax^b L^b + (-\alpha \Delta\mu_r + (1+\gamma) \Delta\mu_F)L} + k_r e^{-\beta \Delta\mu_r L} \right) &= \left(-\alpha \Delta\mu_r + (1 + \gamma) \Delta\mu_F + \frac{\ln k_0 - ax^b L^b}{L} \right) \theta((1 + \gamma) \Delta\mu_F - (\alpha - \beta) \Delta\mu_r) \\ &+ \left(-\beta \Delta\mu_r + \frac{\ln k_r}{L} \right) \theta((\alpha - \beta) \Delta\mu_r - (1 + \gamma) \Delta\mu_F) + o\left(\frac{1}{L}\right) \end{aligned} \quad (\text{S43})$$

Since the x -dependent terms in the right hand sides of the equations above decay with L they vanish in the large L limit. The number of copies with error fraction x is given by the function:

$$f(x) = g(x) + \frac{1}{2L} \ln(2\pi L x(1-x)) + \Delta\mu_r \quad (\text{S44})$$

$$+ \begin{cases} -\Delta\mu_F + o\left(\frac{1}{L}\right) & \text{if } (\alpha - \beta) \Delta\mu_r < \gamma \Delta\mu_F \\ (\alpha - \beta) \Delta\mu_r - (1 + \gamma) \Delta\mu_F + \frac{\ln(k_r/k_0)}{L} + ax^b L^{b-1} + o\left(\frac{1}{L}\right) & \text{if } \gamma \Delta\mu_F < (\alpha - \beta) \Delta\mu_r < (1 + \gamma) \Delta\mu_F \\ o\left(\frac{1}{L}\right) & \text{if } (1 + \gamma) \Delta\mu_F < (\alpha - \beta) \Delta\mu_r, \end{cases} \quad (\text{S45})$$

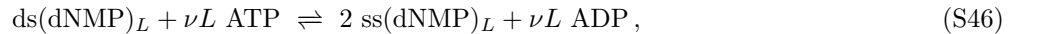
for all values of α , β and γ . In all three cases, in the large L limit the single minimum of function f is x_r .

To achieve sequence-selectivity, it is necessary to have an x -dependent correction to $f - g$ which does not vanish in the large L limit, and which shifts the minimum of f from x_r to a lower error fraction. Since energies scale with L , this is only possible with an exponential dependence of k_j on the number of errors q .

VI. EXAMPLE: DNA REPLICATION

DNA is a double-stranded molecule (dsDNA). Each of its strands is a polynucleotide chain composed of monomeric building blocks called deoxynucleoside monophosphate (dNMP). Those dNMP exist in four versions ($m = 4$), corresponding to the four possible nucleobases that make up the nucleoside: adenine (A), cytosine (C), guanine (G) and thymine (T), and are called dAMP, dCMP, dGMP and dTMP respectively. The two strands are bound together by hydrogen bonds between facing nucleobases according to the basepairing rules: A-T and G-C.

To be copied, the two strands must first be separated into two single-stranded DNA molecules (ssDNA) by breaking the hydrogen bonds. This operation is achieved by the enzyme helicase, which feeds on the fuel adenosine triphosphate (ATP) and releases adenosine diphosphate (ADP). The overall strand separation from start to finish reads:



where $(\text{dNMP})_L$ indicates the chain of dNMP of length L , in its double stranded or single stranded versions. The molecular motor helicase performs two tasks: moving along DNA (translocation) and breaking the hydrogen bonds, which combined consume ν molecules of ATP per basepair unwound. The value of ν may vary depending on the experimental conditions and on the helicase type, but it has been reported to have values of $\nu \approx 2$ [1].

In order for each ssDNA to be copied, the dNMP in the environment must first be converted into deoxynucleoside triphosphate (dNTP). This reaction involves the consumption of 2 ATP molecules which become ADP molecules after losing one phosphate group to the nucleotide [2], and is catalyzed by kinases:



The dNTP can then be incorporated into the growing copy of the ssDNA template. To do so, they are turned back into their monophosphate versions, which releases a pyrophosphate molecule PP_i . The energy released from the hydrolysis

of this PP_i is used to create the high-energy phosphodiester backbone which links the dNMP of the growing copy together. This operation is catalyzed by DNA polymerase and reads:



In our model, the different steps of polymer replication are coarse-grained into a single-step templated assembly process. In the example of DNA replication, the monomers M_i of our model would be the dNMP, the fuel and waste molecules F and W would be the ATP and ADP molecules respectively, and the polymers S_j would be the DNA strands $(\text{dNMP})_L$.

Finally, covalent bonds in the phosphodiester backbone of DNA molecules can also be broken by spontaneous hydrolysis, resulting in two shorter DNA molecules. This reaction is slow but can be catalyzed by deoxyribonuclease enzymes (DNase) without energy expenditure. Repeated hydrolysis can break down DNA molecules into their constitutive dNMP building blocks:



where $N_l \in \{A,C,G,T\}$ is the nucleobase of the nucleoside at position l . In our model, the repeated hydrolyses are coarse-grained into a single-step spontaneous disassembly process.

-
- [1] G. T. Yarranton and M. L. Gefter, Enzyme-catalyzed DNA unwinding: Studies on *Escherichia coli rep* protein, *Proc. Natl. Acad. Sci. U.S.A.* **76**, 1658 (1979).
- [2] I. Lieberman, A. Kornberg, and E. S. Simms, Enzymatic synthesis of nucleoside diphosphates and triphosphates, *J. Biol. Chem.* **215**, 429 (1955).